1521-009X/44/5/700–708$25.00
Drug Metabolism and Disposition

http://dx.doi.org/10.1124/dmd.115.068940
Drug Metab Dispos 44:700–708, May 2016

The ABCG2 Efflux Transporter in the Mammary Gland Mediates Veterinary Drug Secretion across the Blood-Milk Barrier into Milk of Dairy Cows

Hanna Mahnke, Mariana Ballent, Sven Baumann, Fernanda Imperiale, Martin von Bergen, Carlos Lanusse, Adrian L. Lifschitz, Walther Honscha, and Sandra Halwachs

Institute of Pharmacology, Pharmacy and Toxicology, Faculty of Veterinary Medicine (H.M., W.H., S.H.), Institute of Pharmacy, Faculty of Biosciences, Pharmacy and Psychology (S.B.), University of Leipzig, Leipzig, Germany; Laboratorio de Farmacología, Centro de Investigacion Veterinaria de Tandil, (CIVETAN, CONICET-CICPBA), Facultad de Cs. Veterinarias, UNCPBA, Tandil, Argentina (M.B., F.I., C.L., A.L.L.); Department of Molecular Systems Biology, Helmholtz Centre for Environmental Research-UFZ, Leipzig, Germany (S.B., M.vB.); Department of Chemistry and Bioscience, Center for Microbial Communities, University of Aalborg, Aalborg, Denmark (M.vB.)

Received December 11, 2015; accepted March 7, 2016

ABSTRACT

In human and mice ATP-binding cassette efflux transporter ABCG2 represents the main route for active drug transport into milk. However, there is no detailed information on the role of ABCG2 in drug secretion and accumulation in milk of dairy animals. We therefore examined ABCG2-mediated drug transport in the bovine mammary gland by parallel pharmacokinetic studies in lactating Jersey cows and in vitro flux studies using the anthelmintic drug monepantel (MNP) as representative bovine ABCG2 (bABCG2) drug substrate. Animals received MNP (Zolvix, Novartis Animal Health Inc.) once (2.5 mg/kg per os) and the concentrations of MNP and the active MNP metabolite $MNPSO_2$ were assessed by high-performance liquid chromatography. Compared with the parent drug MNP, we detected higher $MNPSO_2$ plasma concentrations (expressed as area under the concentration-versus-time curve). Moreover, we observed $MNPSO_2$ excretion into milk of dairy cows with a high milk-to-plasma ratio of 6.75. In mechanistic flux assays, we determined a preferential time-dependent basolateral-to-apical (B > A) $MNPSO_2$ transport across polarized Madin-Darby canine kidney II cells–bABCG2 monolayers using liquid chromatography coupled with tandem mass spectrometry analysis. The B > A $MNPSO_2$ transport was significantly inhibited by the ABCG2 inhibitor fumitremorgin C in bABCG2- but not in mock-transduced MDCKII cells. Additionally, the antibiotic drug enrofloxacin, the benzimidazole anthelmintic oxfendazole and the macrocyclic lactone anthelmintic moxidectin caused a reduction in the $MNPSO_2$ (B > A) net efflux. Altogether, this study indicated that therapeutically relevant drugs like the anthelmintic MNP represent substrates of the bovine mammary ABCG2 transporter and may thereby be actively concentrated in dairy milk.

Introduction

ABCG2 belongs to the ATP-binding cassette G-subfamily of efflux transporters and is also referred to as breast cancer resistance protein (BCRP) owing to its initial isolation from multidrug-resistant human breast cancer cells (Doyle et al., 1998). The 72-kDa half-transporter ABCG2 is ubiquitously expressed at the apical membrane of important blood-tissue barriers like intestine or placenta, where it plays a protective role by preventing entry of various xenobiotics (Krishnamurthy and Schuetz, 2006). In the human and rodent mammary gland, ABCG2 expression is induced during lactation and represents the major route for active secretion of drugs and toxins into milk (Jonker et al., 2005). As this lactation-induced efflux activity may result in exposure of suckling neonates to potentially harmful substances, ABCG2 in the mammary gland was suggested to be of high toxicological relevance (van Herwaarden and Schinkel, 2006).

In the mammary gland of dairy cows, ABCG2 is also expressed in the apical membrane of alveolar epithelial cells that form the blood-milk barrier. In lactating cows, ABCG2 protein levels were significantly elevated compared with nonlactating animals (Jonker et al., 2005; Lindner et al., 2013). We have recently shown functional ABCG2 efflux activity in primary bovine mammary epithelial cells (Halwachs et al., 2013). Moreover, we cloned the ABCG2 from lactating mammary gland tissues of dairy cows (Wassermann et al., 2013a). The mammary bovine ABCG2 transporter (bABCG2) was stably transduced in MDCKII cells (Wassermann et al., 2013a). We demonstrated the functional bABCG2 efflux activity by transepithelial transport studies (Wassermann et al., 2013b) using the procarcinogen ABCG2 model substrate 2-amino-1-methyl-6-phenylimidazo[4,5-b]pyridine (PhIP)

This work was supported by the German Research Foundation (DFG) [Grant no. HA 7159/1-1] and by the National Council of Scientific and Technical Research [CONICET; Argentina PCI Res. 3060/13].
dx.doi.org/10.1124/dmd.115.068940.

ABBREVIATIONS: ABCG2, ATP-binding cassette subfamily G member 2; ACN, acetonitrile; ANOVA, analysis of variance; AUC, area under the concentration-versus-time curve; ENRO, enrofloxacin; ER, efflux ratio; FTC, fumitremorgin C; HBSS, Hanks' balanced salt solution; HBSS-TP, HBSS transport buffer; HPLC, high-performance liquid chromatography; LC-MS/MS, liquid chromatography coupled with tandem mass spectrometry; LY, Lucifer yellow CH dipotassium salt; MDCKII, Madin-Darby canine kidney II cells; MDCKII-mock, mock-transfected MDCKII; MNP, monepantel; $MNPSO_2$, monepantel sulfone; M/P, milk-to-plasma; MRM, multiple reaction monitoring; MRP, multidrug resistance–associated protein; MXD, moxidectin; OXF, oxfendazole; P_{app}, apparent permeability coefficient; PK, pharmacokinetic; TEER, transepithelial electrical resistance.

(Jonker et al., 2005). Using flux studies, we identified the fluoroquinolone antibiotic enrofloxacin as a bABCG2 substrate (Wassermann et al., 2013b). Moreover, we have shown by indirect Hoechst H33342 efflux assay that the bABCG2 transporter interacts with several important veterinary drugs, including antibiotics or antiparasitics like the anthelmintic drug monepantel (Halwachs et al., 2014).

In dairy animal production, anthelmintic drug therapy is crucial because of severe losses owing to worm infections. Animal losses significantly affect food production, with a resultant economic impact (Behnke et al., 2008). Despite the beneficial use, drug therapy in dairy cows is of public health and food-safety concern owing to the unwanted disposition of milk with drug residues. Antiparasitics including macrolide-like moxidectin (Imperiale et al., 2004) or benzimidazoles (Tsiboukis et al., 2013), are excreted to a varying extent into milk; they have long elimination half-lives and can be recovered in milk samples for several days. In dairy sheep, moxidectin exhibits a high milk-to-plasma (M/P) ratio (Imperiale et al., 2004) that represents an established indicator for active drug secretion into milk (van Herwaarden and Schinkel, 2006). Using *abcg2*$^{-/-}$ mice, it was demonstrated that moxidectin is secreted into murine milk by the ABCG2 efflux transporter (Perez et al., 2009).

In dairy cows, no detailed information is so far available on active drug secretion into milk. Moreover, despite its toxicological relevance, there is as yet no profound data on the role of the ABCG2 efflux transporter in drug disposition in dairy cattle, as well as in active drug residue formation in milk. Hence, the aim of our study was to systematically investigate the functional ABCG2 secretory activity in the bovine mammary gland. In pharmacokinetic studies, the plasma and milk concentration-time profile of the anthelmintic drug and ABCG2 model substrate monepantel (MNP) was therefore assessed in dairy cows. In parallel, functional ABCG2 efflux activity and contribution of ABCG2 to overall drug transport into milk was examined in more detail by in vitro transepithelial MNP flux studies. Therefore, polarized MDCKII cell monolayers expressing bABCG2 served as an adequate in vitro model for the blood-milk barrier (Wassermann et al., 2013b).

Materials and Methods

Reagents. Monepantel sulfone ($MNPSO_2$) was obtained from Witega (Berlin, Germany) at 99.2% purity and 100 μM stock solutions were prepared in dimethyl sulfoxide. Fumitremorgin C (FTC) was purchased from Tocris (Wiesbaden, Germany). Oxfendazole (OXF), moxidectin (MXD), enrofloxacin (ENRO) and Lucifer yellow CH dipotassium salt (LY) were supplied from Sigma-Aldrich (Deisenhofen, Germany).

Pharmacokinetic and Milk Secretion Experiments in Dairy Cows. Lactating female Jersey cows (~600 kg b.wt.), 2–3 years of age, were maintained on a dairy farm around Tandil, Argentina. Six clinically healthy animals received a single oral dose of monepantel (Zolvix; Novartis Animal Health Inc., Eli Lilly and Company/Elanco, Greenfield, IN). Blood samples were taken from the jugular vein in heparinized blood collection tubes at 3, 8, 24, 33, 57, 81, 129, 157, and 177 hours post-treatment. Plasma was separated by centrifugation at 2000*g* for 20 minutes, and the recovered plasma transferred into vials. Milk samples were collected from 8 hours up to 200 hours post-treatment, at 24-hour time intervals following the milking routine. At each time point, a milk sample was collected by hand milking before the complete mechanical milking of each animal. Plasma and milk samples were stored at –20°C until high-performance liquid chromatography (HPLC) analysis. Animal procedures and management protocols were carried out according to the Animal Welfare Policy (Academic Council Resolution 087/02) of the Faculty of Veterinary Medicine, Universidad Nacional del Centro de la Provincia de Buenos Aires (UNCPBA), Tandil, Argentina (http://www.vet.unicen.edu.ar) and approved by the animal welfare committee.

Analytical Procedures. The extraction of MNP and $MNPSO_2$ from spiked and experimental plasma and milk samples was carried out using the technique described by Karadzovska et al. (2009), and modified by Lifschitz et al. (2014). Drug was extracted from plasma and milk by addition of 0.5 ml water and 2.0 ml acetonitrile under a high-speed vortexing shaker (Multi-Tube Vortexer; VWR Scientific Products, West Chester, PA) for 15 minutes. After centrifugation (BR 4i Centrifuge; Jouan, Saint Herblain, France) at 2000*g* for 15 minutes at 10°C to allow phase separation, the clear supernatant was transferred to a 10-ml plastic tube and mixed with 6 ml of pure water. The mixture was vortexed for 5 seconds and transferred to a polymeric sorbent solid-phase extraction cartridge (Strata-X 33-μm Polymeric sorbent 60 mg; Phenomenex Torrance, CA) previously conditioned with 1.0 ml acetonitrile and 1.0 ml water. All samples were applied and then sequentially washed with 2.0 ml of acetonitrile/water (30:70, v/v), dried with air for 1 minute, and eluted with 1.5 ml of acetonitrile. The eluted volume was evaporated (40°C) to dryness in a vacuum concentrator (Speed Vac, Savant, Los Angeles, CA), and then reconstituted with 250 μl of mobile phase.

For HPLC analysis, 50 microliters of each sample were injected in a Shimadzu chromatography system (Shimadzu Corporation, Kyoto, Japan), with two LC-10AS solvent pumps, an automatic sample injector (SIL-10A), a UV-visible spectrophotometric detector (SPD-10A UV), a column oven (Eppendorf TC-45, Eppendorf, Madison, WI) set at 30°C, and a CBM-10A data integrator. Data and chromatograms were collected and analyzed using the Class LC10 software (SPD-0A; Shimadzu Corporation). A C18 reversed-phase column (5 μm, 4.6 mm × 250 mm; Kromasil; Eka Chemicals, Bohus, Sweden) was used for separation. Elution of MNP from the stationary phase was carried out at a flow rate of 0.8 ml min^{-1} (MNP) and 1.2 ml min^{-1} using acetonitrile/methanol/water (60:8:32, v/v/v). The detection of drugs and metabolites was done at a wavelength of 230 nm.

Pharmacokinetic Calculations and Statistical Analysis. MNP and $MNPSO_2$ plasma concentration profiles as well as $MNPSO_2$ milk- and plasma-concentration profiles obtained after treatment of each individual animal were fitted with the Solution 2.0 software (PK Solutions, Ashland, OH). Pharmacokinetic parameters were determined using noncompartmental analysis, and maximum plasma and milk concentrations (C_{max}) were read from the plotted concentration-time curve of each individual animal. The area under the concentration-versus-time curve (AUC) was calculated by the trapezoidal rule (Perrier and Gibaldi, 1982). Statistical analysis of the data were carried out using Microsoft Excel (Office 2000) and Sigma Plot 11.0 software (Systat Software, San Jose, CA). Pharmacokinetic parameters are reported as mean ± S.D. Mean AUC for MNP and $MNPSO_2$ were statistically compared using one-way analysis of variance (ANOVA) followed by the Fisher's least significant difference (LSD) post-hoc test. Statistical significance was assumed at P values ≤ 0.05.

Cell Culture. Characterization and culture conditions of bovine ABCG2 (bABCG2)-expressing or mock-transfected MDCKII (MDCKII-mock) cells has been delineated recently (Wassermann et al., 2013b). Polarized monolayers were obtained by culture on Transwell clear polyester inserts (0.33- cm^2 growth area, 0.4-μm pore size; Corning, Wiesbaden, Germany). MDCKII-bABCG2 (6×10^4 cell/ml) or MDCKII-mock cells (12.5×10^4 cells/ml) were suspended in 0.3 ml of complete growth medium and added to the inner chamber, which was inserted into the outer chamber containing 0.7 ml of culture medium. Formation of functional cell monolayers was followed by measurement of transepithelial electrical resistance (TEER) using a low-impedance volt-ohm meter equipped with a chopstick electrode (Millipore, Schwalbach, Germany).

Transepithelial Transport Studies. Flux experiments were performed in 5-day-old cultures corresponding to 48 hours after cells had reached clone-specific peak TEER values (Wassermann et al., 2013b). Before the start of flux studies, cells were incubated (2 hours) with medium with or without FTC (10 μM) or incubated (4 hours) with medium with or without OXF (10 μM), MXD (0.6 μM), or ENRO (20 μM). Selected concentrations of all tested drugs including $MNPSO_2$ (1 μM) corresponded to the 10-fold maximum therapeutic plasma concentration (C_{max}) in dairy ruminants (Karadzovska et al., 2009). Cell monolayers were then washed with Hanks' balanced salt solution (HBSS) supplemented with 20 mM glucose and 20 mM HEPES (pH 7.8). Transport experiments were started by addition of HBSS transport buffer (HBSS-TP) containing $MNPSO_2$ (1 μM dissolved in 1% dimethyl sulfoxide) with or without FTC (10 μM), OXF (10 μM), MXD (0.6 μM), or ENRO (20 μM) to either the apical (for determination of apical-to-basolateral transport, A > B) or basolateral (for determination of basolateral-to-apical transport, B > A) compartment. Cells were then incubated at 37°C with 5% CO_2, and aliquots of 10 μl were taken at 1, 2, 3, or 4 hours. For 4°C experiments, flux studies were performed as delineated above using cold HBSS-TP and incubation of cells at 4°C. In general, transport buffer with or without inhibitor or drug was replaced in the respective compartment to avoid

hydrostatic pressure. The samples were transferred to vials and diluted (1:100) with 50% acetonitrile (ACN) (VWR, Darmstadt, Germany) and 50% ultrapure water (Milli-Q system plus; Millipore, Schwalbach, Germany). After vigorous vortexing the samples were stored at –80°C until liquid chromatography coupled with tandem mass spectrometry (LC-MS/MS) analysis.

The vectorial flux of $MNPSO_2$ across MDCKII-bABCG2 and MDCKII-mock monolayers was calculated as the apparent permeability coefficient (P_{app}) in centimeters per second using the following equation: P_{app} (cm/s) = Flux (pmol/h)/3600 (s/h)/S (pmol/cm^3)/0.33 (cm^2), where S defines the substrate concentration initially added to the respective compartment (Kneuer et al., 2005). $MNPSO_2$ efflux ratios (ER) were then calculated as follows: ER = P_{app} B > A/P_{app} A > B. After each experiment the tightness of cell monolayers was verified by the paracellular flux marker LY (Irvine JD et al., 1999). Therefore, cells were washed with HBSS-TP, and 200 μl of transport buffer containing LY (60 μM) was added to the apical compartment. Cells were incubated at 37°C with 5% CO_2 for 1 hour. Aliquots from the apical (50 μl) and from the basolateral (200 μl) compartment were then taken, transferred to 96-well plates (Brand, Wertheim, Germany), and LY was quantified using a fluorescence plate reader (480/530 nm; Genios, Tecan, Crailsheim, Germany). The A > B P_{app} (nm/s) values for LY were calculated according to the following equation: $P_{app} = (dQ/dt)/(C_0{*}A)$, where dQ/dt is the permeability rate, C_0 is the initial concentration in the donor compartment and A is the surface area of the filter.

Quantification of $MNPSO_2$ Using UPLC-MS/MS. All analyses were performed on a UltiMate 3000 RSLC (ThermoFisher Scientific, Dreieich, Germany), a 5500 QTRAP triple quadrupole LC-MS/MS mass spectrometer (AB Sciex, Darmstadt, Germany) equipped with a TurboIonSpray source. Liquid chromatography was performed in gradient elution mode using Acquity C18, (50 mm × 2.1 mm, 1.7 μm; Waters, Milford, MA) at 60°C with eluent A (water, 0.1% formic acid) and eluent B (ACN, 0.1% formic acid) with a flow rate of 500 μl/min. The injection volume of each sample was 5 μl. A linear gradient of eluent B was used: 0 minutes, 30%; 0.7 minutes, 30%; 3.7 minutes, 95%; 4.6 minutes, 95%; 4.7 minutes, 30%; 5.6 minutes, 30%. For $MNPSO_2$ quantification MS was operated in negative ion and multiple reaction monitoring (MRM) modes. Optimized electrospray ionization MS/MS–dependent parameters were as following: ion spray voltage –4.3 kV and ion source gas 1, ion source gas 2, curtain gas, and collision gas, 40, 50, 20, "medium" (arbitrary) units, respectively. The source temperature was maintained at 450°C. The MRM-assay was performed by monitoring the precursor ion of *m/z* 504.2 ([M-H]$^-$) together with three characteristic product ions at *m/z* 186.0, 166.0, and 138.0. Optimized declustering potential, entrance potential, and collision cell exit potential for MRM experiments were set to 100 V, 10 V, and 13 V respectively. Collision energies were also optimized as follows for the above mentioned transitions: 25 V, 35 V, and 35 V. Standard solutions were prepared by appropriate dilution of the stock solutions with water/ACN (1:1 v/v). The concentrations of $MNPSO_2$ in these standards ranged from 0.01 to 10 nM. The calibration curves were obtained by using weighted (1/*x*) least-squares regression analysis. To evaluate intra- and interday imprecision, aliquots ($n = 9$) at low and high concentrations (100 pM and 10 nM) were analyzed using LC-MS/MS over a period of three consecutive days. The limit of detection (LOD) and lower limit of quantification (LLOQ) was considered to be at a signal-to-noise ratio of 3 and 10, respectively, and was determined using lowest calibration standard at 10 pM.

Statistics. Statistical analyses of the flux study data were carried out using Microsoft Excel software (Office 2000) and Sigma Plot 11.0 (Systat Software, San Jose, CA). Differences between mean values of ABCG2-transduced MDCKII cells compared with the mock control, as well as differences between pretreated MDCKII cultures compared with untreated control cells, were assessed by two-way ANOVA followed by a Fisher's LSD post-hoc test. Statistical significance was assumed at P values of ≤ 0.05.

Results

Plasma and Milk Pharmacokinetics of MNP and $MNPSO_2$ in Dairy Cows. To elucidate the role of ABCG2 in carrier-mediated drug concentration in milk, we initially performed pharmacokinetic studies in dairy cows. Here, we investigated the plasma and milk concentration-time profile of the ABCG2 drug substrate MNP. Using HPLC analysis the quantification limits of MNP and $MNPSO_2$ in plasma and milk were 4 ng/ml and 25 ng/ml, respectively. The recovery of both analytes was between 84 and 97%. The coefficient of variation (CV) of HPLC analysis for MNP and $MNPSO_2$ was between 1 and 7.63% (plasma) and 1.44 and 12.5% (milk).

Following a single oral MNP administration, we measured MNP and its active metabolite $MNPSO_2$ in plasma samples. A full set of kinetic parameters is shown in Table 1. $MNPSO_2$ was the main analyte recovered from plasma and could be assessed over the whole sampling period up to 177 hours, whereas MNP was measured only at early time points up to 36 hours (Fig. 1A). Compared with the MNP AUC values of 0.94 ± 0.17 μg-h/ml, significantly higher AUC values of 21.2 ± 9.2 μg-h/ml were detected for the $MNPSO_2$ derivative in plasma (Table 1). In milk samples, we detected MNP up to 33 hours (not shown) and $MNPSO_2$ up to 177 hours post-administration of a single oral MNP dose (Fig. 1B). The percentage of the fraction of dose excreted in milk was 0.09% for MNP and 2.79% for $MNPSO_2$. The AUC value of $MNPSO_2$ in milk (123.8 ± 43.3 μg-h/ml) (Table 1) was significantly higher than the AUC value obtained in plasma samples. Using these AUC values, an $MNPSO_2$ milk-to-plasma (M/P) ratio of 6.75 ± 3.54 was calculated (Table 1).

Validation of the Barrier Function of Polarized MDCKII Cell Monolayers. To investigate ABCG2-mediated drug transport across the normal bovine blood-milk barrier, MDCKII cells stably expressing ABCG2 from the bovine lactating mammary gland (bABCG2) (Wassermann et al., 2013a) were grown on microporous filter inserts. We confirmed the barrier function of 5-day-old MDCKII-bABCG2 monolayers by TEER measurements as defined recently (Wassermann et al., 2013b). Additionally, tightness of cell monolayers was validated after each experiment by permeability of the paracellular flux marker LY (Irvine et al., 1999). The mean LY P_{app} value in all experiments was 4.13 ± 0.64 nm/s. Moreover, in each flux study the recovered LY concentration in the basolateral compartment corresponded to ≤1% of the initially applied LY concentration in the apical compartment. TEER values and LY permeability served as internal criteria for the barrier function of MDCKII monolayers in all subsequent flux experiments.

Time-Dependent and Vectorial Transport of $MNPSO_2$ across MDCKII-bABCG2 and MDCKII-Mock Monolayers. In the initial pharmacokinetic studies in dairy cows, the MNP metabolite monepantel sulfone was the main analyte recovered from plasma and milk. Hence, in all in vitro transepithelial transport studies functional bABCG2 efflux activity was examined using $MNPSO_2$ as ABCG2 model substrate. Therefore, major analytical parameters of LC-MS/MS–based quantification of $MNPSO_2$ were determined. Linearity for the quantification was tested and given in the calibration range. Potential matrix effects resulting from cell culture medium of 100-fold diluted samples were

TABLE 1

Pharmacokinetic parameters for MNP and $MNPSO_2$ in plasma and milk following a single oral 2.5 mg/kg dose of MNP to dairy cows

Data are reported as mean ± S.D.; n = 6. *Mean kinetic parameters significantly different from those obtained for MNP at $P < 0.05$.

Kinetic Parameters	MNP (Plasma)	$MNPSO_2$ (Plasma)	$MNPSO_2$ (Milk)
$AUC0_{0-t}$ (μg-h/ml)	0.94 ± 0.17	21.2 ± 9.20*	123.8 ± 43.3
C_{max} (μg/ml)	0.08 ± 0.03	0.40 ± 0.13*	2.65 ± 0.91
T_{max} (h)	3.00 ± 0.00	5.50 ± 2.74	8.00 ± 0.00
$T_{1/2\ el}$ (h)	12.1 ± 5.70	73.1 ± 51.4*	60.3 ± 15.2
Ratio of the AUC $MNPSO_2$/MNP		23.1 ± 10.5	
$MNPSO_2$ milk-to-plasma ratio (AUC)		6.75 ± 3.54	

AUC_{0-t}, area under the concentration-versus-time curve. C_{max}, peak plasma concentration. T_{max}, time to peak plasma concentration. $T_{1/2\ el}$, elimination half-life.

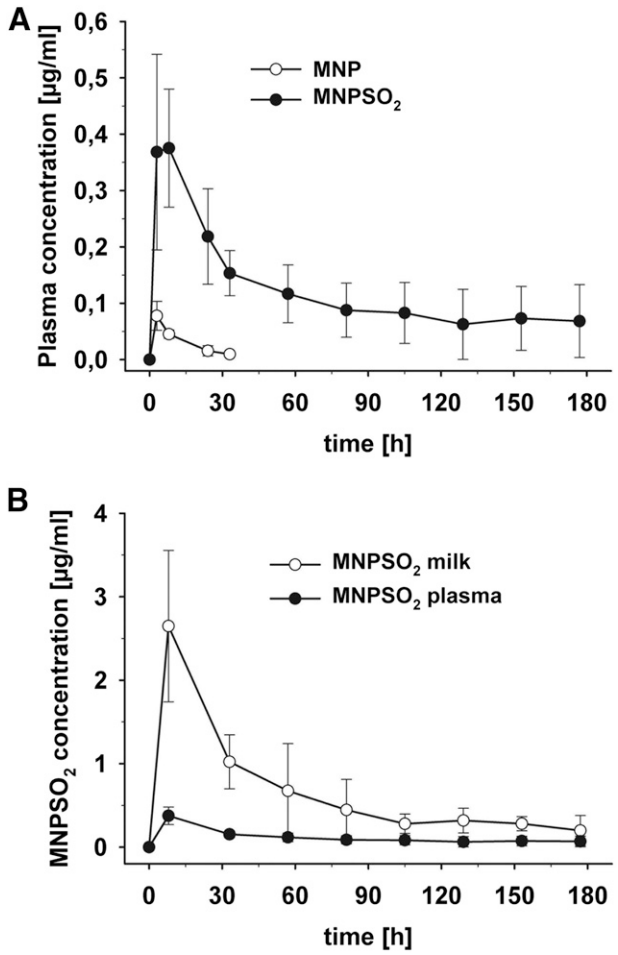

Fig. 1. Comparative (mean ± S.D., n = 6) MNP and $MNPSO_2$ plasma concentration profiles (A) and comparative (mean ± S.D., n = 6) $MNPSO_2$ concentration profiles in milk and plasma (B) obtained after the oral administration of MNP (2.5 mg/kg once) to dairy cows.

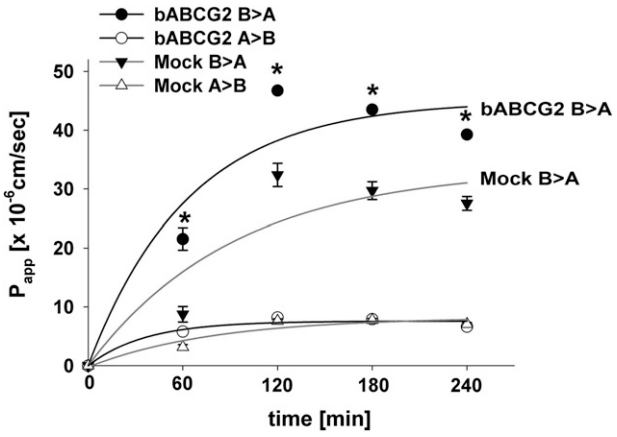

Fig. 2. Time-dependent vectorial transepithelial transport of $MNPSO_2$ across MDCKII-bABCG2 and MDCKII-mock cell monolayers. Polarized MDCKII monolayers were cultured on porous membrane filters for 5 days. Transport experiments were initiated by addition of $MNPSO_2$ (1 μM) in the respective compartment, and aliquots were taken at 60, 120, 180, and 240 minutes as described in *Materials and Methods*. Vectorial $MNPSO_2$ transport across MDCKII-bABCG2 monolayers was measured as the apically directed B > A or basolaterally directed A > B flux of $MNPSO_2$ and expressed in P_{app} values in centimeters per second. Parallel $MNPSO_2$ flux studies in mock-transfected MDCKII cells served as in internal control. Values are mean ± S.E.M. (*$P < 0.05$ significantly different from B > A $MNPSO_2$ flux in mock-control cells; two-way ANOVA, Fisher's LSD post-hoc test; data are shown from nine monolayers, each with n = 3, as technical replicates).

tested and not observed. LOD for $MNPSO_2$ was calculated at 2.7 pM, LLOQ at 9.0 pM. Furthermore the intra- and interassay imprecision was determined at two different concentrations (n = 9) and revealed variances below 10%. In detail, intraday variances were calculated with 6.5% and 2.4% at low and high concentration. Interday variances were slightly higher with 7.6% and 3.5%.

MDCKII-bABCG2 and MDCKII-mock control cells were grown to confluent polarized monolayers on microporous membrane filters and the vectorial and time-dependent transport of $MNPSO_2$ (1 μM) across 5-day-old cell monolayers was determined. We then calculated P_{app} values for the apically (B > A) or the basolaterally (A > B) directed transport rate as described in *Material and Methods*. In both MDCKII clones, the B > A–directed $MNPSO_2$ transport was significantly higher compared with the A > B $MNPSO_2$ flux (Fig. 2). We observed an initial increase in the B > A $MNPSO_2$ flux rate with peak P_{app} values at 2 hours in MDCKII-bABCG2 cells of $46.7 \pm 0.5 \times 10^{-6}$ cm/s. This was followed by a slight drop and a steady-state plateau phase in $MNPSO_2$ P_{app} values of $39.3 \pm 0.5 \times 10^{-6}$ cm/s up to 4 hours of transport measurements. Compared with mock-transfected control cells, we detected a significantly higher time-dependent $MNPSO_2$ flux rate in bABCG2-transduced MDCKII cells, with on average 1.5-fold higher $MNPSO_2$ P_{app} values (Fig. 2).

To examine passive diffusion of $MNPSO_2$ across MDCKII cell monolayers, we measured the bidirectional time-dependent $MNPSO_2$ transport at 4°C across MDCKII-bABCG2 and MDCKII-mock cell monolayers. Compared with transport measurements at 37°C, P_{app} values for the apically (B > A) directed $MNPSO_2$ transport in the bABCG2 clone dramatically decreased to $3.77 \pm 0.64 \times 10^{-6}$ cm/s and $6.41 \pm 0.4 \times 10^{-6}$ cm/s at 2 hours and at 4 hours, respectively. Moreover at 4°C, the time-dependent B > A– and the A > B–directed $MNPSO_2$ flux did not significantly differ (not shown). In mock-control cells, B > A $MNPSO_2$ P_{app} values at 2 hours and 4 hours were $4.62 \pm 1.2 \times 10^{-6}$ cm/s and $5.56 \pm 1.2 \times 10^{-6}$ cm/s, respectively, and showed no significant difference compared with MDCKII-bABCG2 cells.

Effect of FTC and Enrofloxacin on Transepithelial $MNPSO_2$ Transport. To test the specificity of bABCG2-mediated $MNPSO_2$ transport, we measured the transepithelial $MNPSO_2$ flux rate across MDCKII-bABCG2 and MDCKII-mock monolayers in the presence or absence of the specific ABCG2 inhibitor FTC (Rabindran et al., 2000) and the bovine ABCG2 drug substrate enrofloxacin (Wassermann et al., 2013b).

Compared with the untreated bABCG2-MDCKII cells, FTC caused a significant decrease in the B > A–directed $MNPSO_2$ transport (Fig. 3A). In contrast, FTC had no significant effect on the $MNPSO_2$-directed B > A transport in mock-control cells (Fig. 3B). In the presence of FTC, we observed a comparable B > A $MNPSO_2$ flux rate (4 hours) in bABCG2-transduced and mock-control cells with P_{app} values of $45.53 \pm 1.2 \times 10^{-6}$ cm/s and $51.42 \pm 1.1 \times 10^{-6}$ cm/s, respectively. In both cell lines, basolaterally (A > B) directed $MNPSO_2$ transport was not significantly affected by FTC (Fig. 3). We additionally calculated B > A/A > B efflux ratios for transepithelial $MNPSO_2$ transport. As shown in Fig. 3C, the ER in untreated MDCKII-bABCG2 cells was significantly higher compared with the mock-control. At 120 minutes and 240 minutes, FTC caused a significant reduction in $MNPSO_2$ efflux ratios in bABCG2-transduced cells but not in mock cells (Fig. 3C).

To further specify $MNPSO_2$ transport by bABCG2, we tested transepithelial $MNPSO_2$ flux in both MDCKII clones in the presence of ENRO. In bABCG2-transduced MDCKII cells, addition of ENRO resulted in a significant decrease in P_{app} values for the B > A–directed

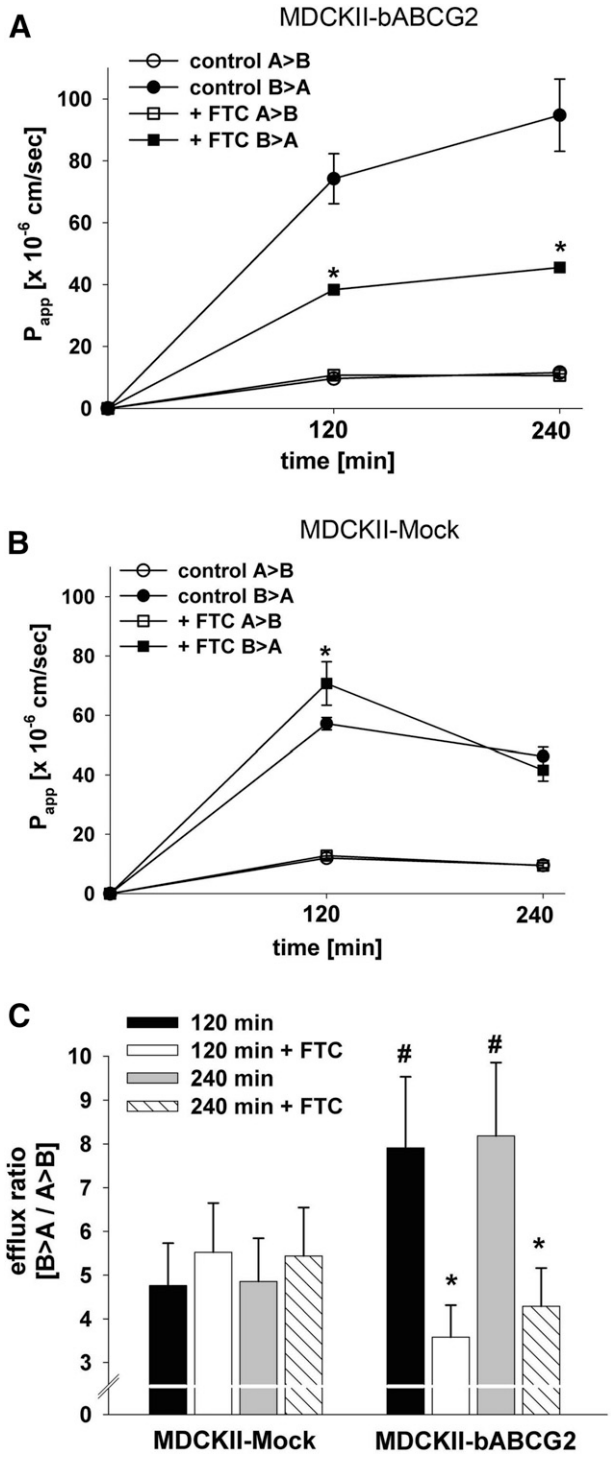

Fig. 3. Effect of FTC on transepithelial $MNPSO_2$ transport in MDCKII-bABCG2 and -mock cells. Both cell lines were grown on porous membrane filters, and 5-day-old polarized cell monolayers were pretreated with 10 μM FTC for 2 hours. Transport experiments were then initiated by addition of $MNPSO_2$ (1 μM) in the respective donor compartment as delineated in *Materials and Methods*. For transport experiments, MDCKII-bABCG2 cells (A) or MDCKII-mock control cells (B) were incubated with $MNPSO_2$ in the presence or absence of 10 μM FTC and samples were taken at 120 minutes or 240 minutes. P_{app} values in cm/s were obtained as described in the legend for Fig. 2, and P_{app} values as well as transcellular $MNPSO_2$ efflux ratios [P_{app} B > A/A > B] in both MDCKII clones (C) were calculated as described in *Materials and Methods*. Values are mean ± S.E.M. (*$P < 0.05$ significantly different to untreated MDCKII-bABCG2 cells, #$P < 0.05$ significantly different to MDCKII-mock cells; two-way ANOVA, Fisher's LSD post-hoc test; data are presented from eight monolayers, each with $n = 3$, as technical replicates).

$MNPSO_2$ transport at 120 minutes and 240 minutes compared with the untreated control (Fig. 4A). In the mock cell line, ENRO caused an increase in the B > A–directed $MNPSO_2$ transport at 120 minutes and 240 minutes compared with the untreated control (Fig. 4B). In both cell lines, basolaterally (A > B) directed $MNPSO_2$ transport was not significantly affected by ENRO (Fig. 4). In the presence of ENRO, the $MNPSO_2$ efflux ratios in bABCG2-transduced cells were significantly reduced (Fig. 4C). In contrast, we observed no significant changes in the ER for $MNPSO_2$ in MDCKII-mock cells (Fig. 4C).

Effect of Oxfendazole and Moxidectin on Transepithelial $MNPSO_2$ Transport. To further specify the contribution of ABCG2 in drug transport in the bovine mammary gland, we examined the effect of the anthelmintic drug OXF and the antiparasitic drug moxidectin on the transepithelial $MNPSO_2$ flux across MDCKII-bABCG2 and MDCKII-mock monolayers.

Compared with the untreated MDCKII-bABCG2 cells, addition of OXF (10 μM) caused a significant decrease in the time-dependent B > A–directed $MNPSO_2$ transport (Fig. 5A) to the level of untreated MDCKII-mock control cells (Fig. 5B). In mock cells, OXF led to an increase in P_{app} values for the B > A–directed $MNPSO_2$ flux (Fig. 5B). However, the overall time-dependent $MNPSO_2$ efflux ratios in these cells were not significantly changed in the OXF-treated in relation to untreated mock cells (Fig. 5C). In bABCG2-transduced cells, the ER for $MNPSO_2$ was significantly higher compared with mock-control cells (Fig. 5C). As illustrated in Fig. 5C, OXF caused a significant reduction in the ER compared with untreated MDCKII-bABCG2 cells.

As illustrated in Fig. 6A, the time-dependent B > A–directed $MNPSO_2$ transport was significantly reduced in MXD-treated compared with -untreated MDCKII-bABCG2 cells. In relation to untreated mock cells, MXD (0.6 μM) caused a slight increase in the time-dependent P_{app} values for the B > A–directed $MNPSO_2$ flux (Fig. 6B). The time-dependent $MNPSO_2$ efflux ratios in MDCKII-bABCG2 cells were significantly higher compared with mock-control cells (Fig. 6C). Incubation with MXD only resulted in decreased efflux ratios for $MNPSO_2$ in MDCKII-bABCG2 cells, whereas no inhibition occurred in MDCKII-mock cells (Fig. 6C). Treatment of both MDCKII clones with OXF (Fig. 5) or MXD (Fig. 6) had no significant effect on the basolaterally directed (A > B) $MNPSO_2$ transport and $MNPSO_2$ efflux ratios.

Discussion

In preliminary studies, the interaction of several drugs, including the anthelmintic drug MNP with the bovine mammary ABCG2 (bABCG2) efflux transporter was shown (Wassermann et al., 2013a; Halwachs et al., 2014). However, the involvement of ABCG2 in drug disposition in dairy cattle as well as in active drug residue formation in milk, remained poorly understood. In this study, therefore, we aimed to systematically address this problem by combined in vivo pharmacokinetic (PK) and mechanistic in vitro flux studies. In all experiments, $MNPSO_2$ served as ABCG2 model substrate.

This is the first report on the pharmacokinetics of the novel significant anthelmintic drug MNP in cattle. In agreement with previous PK studies in sheep (Karadzovska et al., 2009; Lifschitz et al., 2014), we observed a very rapid in vivo metabolism of MNP after oral drug administration. The sulfone metabolite $MNPSO_2$ was the main metabolite recovered from plasma samples, with a persistence in the bovine bloodstream significantly longer than that of the parent drug. Our results are in line with the MNP metabolic pattern reported earlier in sheep (Karadzovska et al., 2009; Hosking et al., 2010; Lifschitz et al., 2014). Using primary ovine hepatocytes, various phase I and phase II metabolites could be determined (Stuchlikova et al., 2013). However, as observed in the current PK study in dairy cows, the main MNP

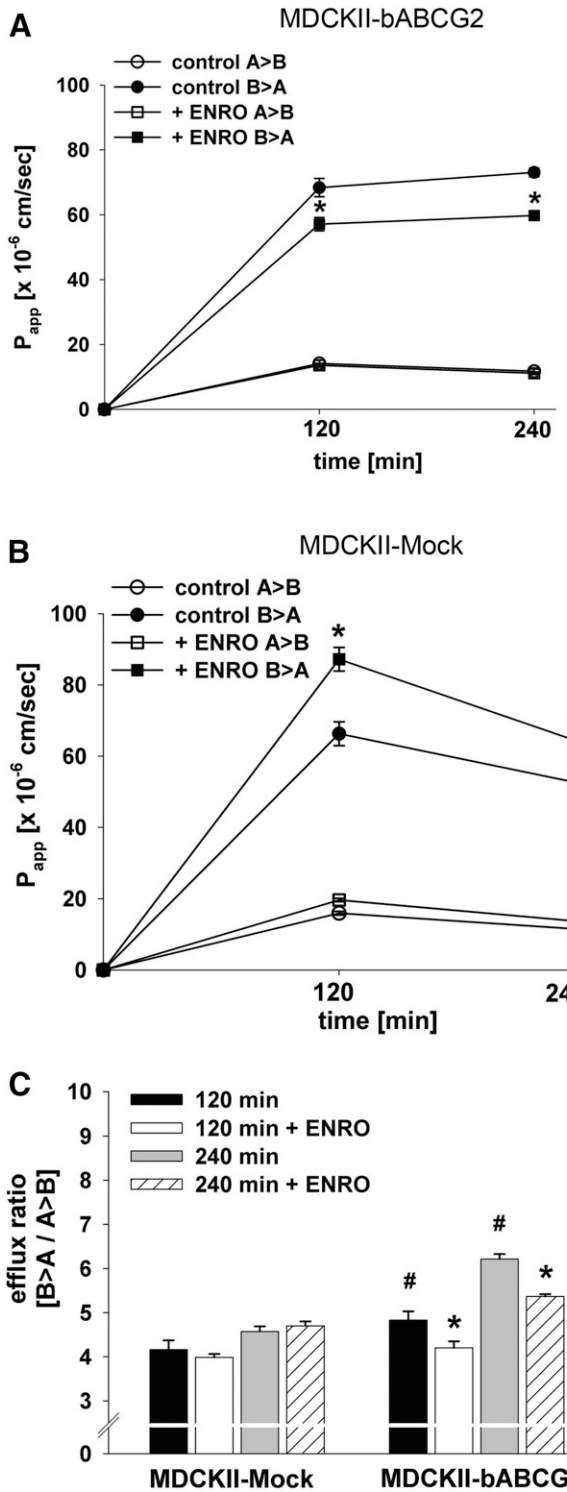

Fig. 4. Influence of ENRO on transcellular $MNPSO_2$ transport in MDCKII-bABCG2 and -mock cells. Five-day-old polarized MDCKII monolayers were pretreated with ENRO (20 μM) for 4 hours. Transport experiments were initiated by addition of $MNPSO_2$ (1 μM) and both cell lines were incubated in the absence or presence of ENRO for 120 minutes or 240 minutes. $MNPSO_2$ P_{app} values in MDCKII-bABCG2 (A) and -mock (B) cells as well as efflux ratios (C) for $MNPSO_2$ efflux ratios were determined as described in the legend for Fig. 2. The results represent the mean ± S.E.M. ($^*P < 0.05$ significantly different to untreated MDCKII-bABCG2 cells, $^{\#}P < 0.05$ significantly different to MDCKII-mock cells; two-way ANOVA, Fisher's LSD post-hoc test; data are shown from six monolayers, each with $n = 3$, as technical replicates).

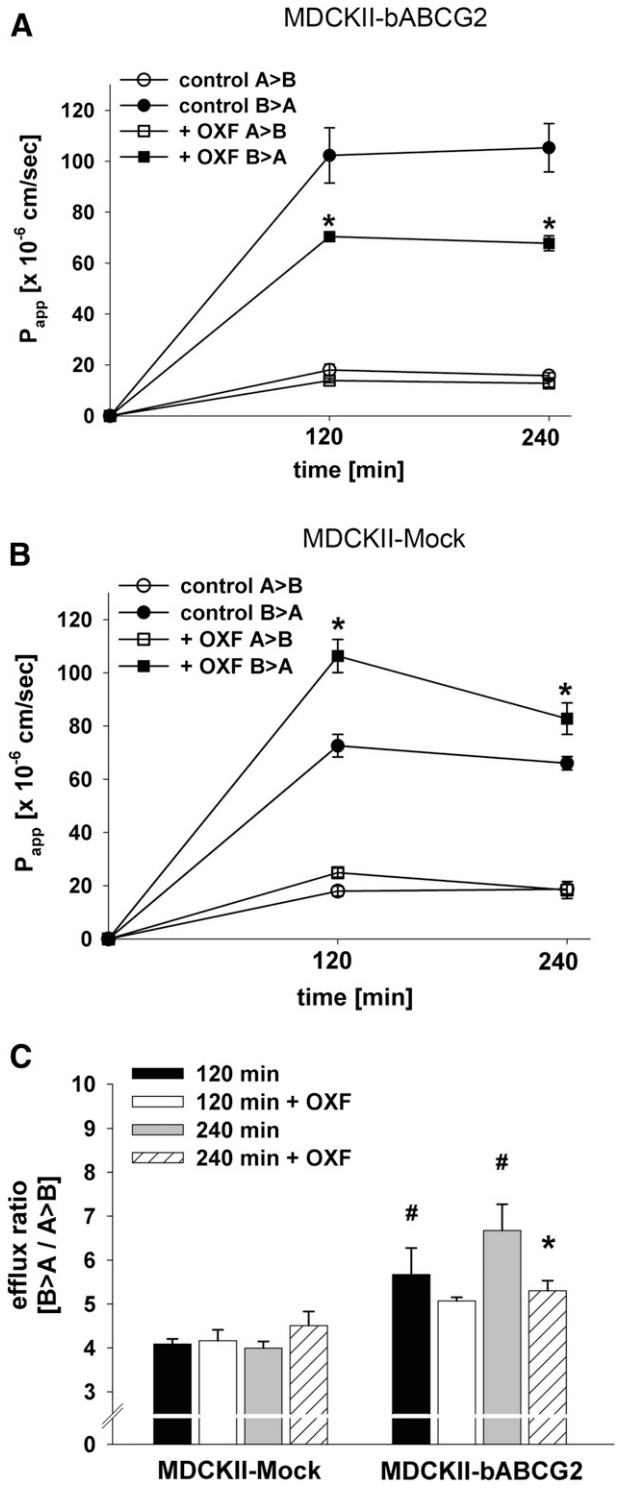

Fig. 5. Effect of OXF on transcellular $MNPSO_2$ transport in MDCKII-bABCG2 and -mock cells. Five-day-old polarized cell monolayers were pretreated with OXF (10 μM) for 4 hours. Transport experiments were initiated by addition of $MNPSO_2$ (1 μM), and both cell lines were incubated in the absence or presence of OXF for 120 minutes or 240 minutes. $MNPSO_2$ P_{app} values in MDCKII-bABCG2 (A) or -mock (B) cells as well as $MNPSO_2$ efflux ratios (C) were obtained as delineated in the legend for Fig. 2. The data represent the mean ± SEM ($^*P < 0.05$ significantly different to untreated MDCKII-bABCG2 cells, $^{\#}P < 0.05$ significantly different to MDCKII-mock cells; two-way ANOVA, Fisher's LSD post-hoc test; data are shown from four monolayers, each with $n = 3$, as technical replicates).

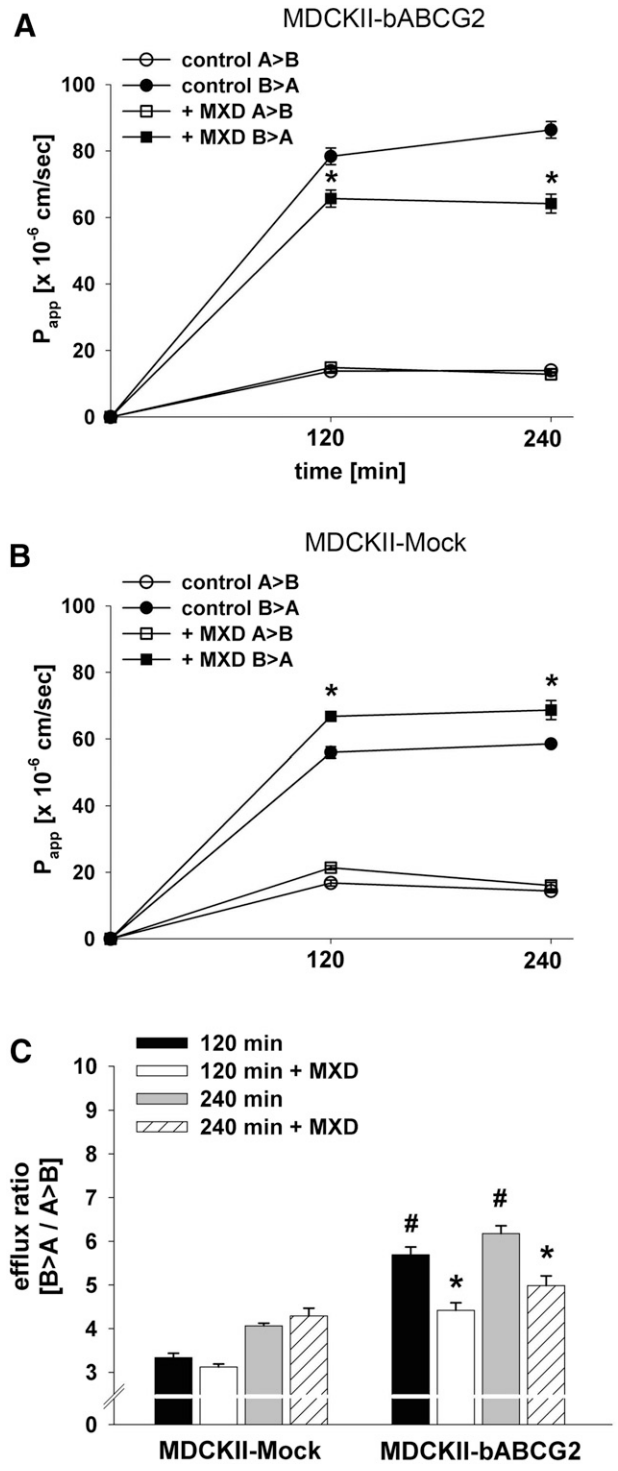

Fig. 6. Influence of moxidectin on transepithelial $MNPSO_2$ transport in MDCKII-bABCG2 and -mock cells. MDCKII clones were cultured on porous membrane filters for 5 days, and polarized cell monolayers were pretreated with MXD (0.6 μM) for 4 hours. Transport experiments were initiated by addition of $MNPSO_2$ (1 μM) and both cell lines were incubated in the absence or presence of MXD for 120 minutes or 240 minutes. $MNPSO_2$ P_{app} values in MDCKII-bABCG2 (A) or -mock (B) cells as well as $MNPSO_2$ efflux ratios (C) were determined as described in the legend for Fig. 2. The data represent the mean ± S.E.M. ($^*P < 0.05$ significantly different to untreated MDCKII-bABCG2 cells, $^{\#}P < 0.05$ significantly different to MDCKII-mock cells; two-way ANOVA, Fisher's LSD post-hoc test; data are shown from six monolayers, each with $n = 3$, as technical replicates).

metabolite determined in ovine plasma in vivo was restricted to $MNPSO_2$ (Lifschitz et al., 2014).

In milk of dairy cows, $MNPSO_2$ was also the main analyte and exhibited a significantly longer persistence compared with MNP. A similar observation was made recently in lactating sheep (EMA, 2013). In relation to plasma, significantly higher $MNPSO_2$ concentrations were recovered in milk, as illustrated by the high $MNPSO_2$ M/P ratio. The M/P ratio represents a useful tool to identify substances that are actively transported and subsequently concentrated in milk (Alvarez et al., 2006; van Herwaarden and Schinkel, 2006). This might represent an undesirably high contamination of cow's milk as the detected C_{max} of $MNPSO_2$ in milk (C_{max}: 2.56 ± 0.91 μg/ml) was higher than the established maximum residue limit in milk of sheep (EMA, 2013). Besides, transfer into milk may generally depend on the physicochemical drug properties like ionization, lipophilicity, or protein binding (Ito and Lee, 2003). However, previous studies using *abcg2*$^{-/-}$ mice demonstrated a strong correlation between high M/P ratios and active ABCG2-mediated drug secretion into milk, including the chemotherapeutic drug topotecan or the antiulcerative drug cimetidine (Jonker et al., 2005). Hence, in regard to the high $MNPSO_2$ M/P ratio in dairy cows, transport of $MNPSO_2$ into milk by the bABCG2 efflux transporter is also very probable.

To examine the contribution of bovine mammary ABCG2 in veterinary drug secretion and concentration in milk in more detail, we performed mechanistic transepithelial transport studies. In this study, we used polarized MDCKII monolayers stably expressing ABCG2 from the lactating bovine mammary gland (Wassermann et al., 2013a). The MDCKII-bABCG2 cell line represents an adequate in vitro model to elucidate the overall contribution of bABCG2 in drug transport across pharmacological tissue barriers (Hegedus et al., 2009; Wassermann et al., 2013b) like the blood-milk barrier. However, using the MDCKII cell line, endogenous expression of efflux transporters such as canine ABCG2 must be considered (Hegedus et al., 2009). We therefore included mock-transfected MDCKII cells (Wassermann et al., 2013a) in all flux studies to consider the effect of intrinsic transporters on transepithelial $MNPSO_2$ transport in MDCKII-bABCG2 cells. The formation of the MDCKII monolayer barrier function was confirmed using the established paracellular flux marker LY (Cho et al., 1989; Irvine et al., 1999). Generally, LY permeability across polarized MDCKII-bABCG2 monolayers was low, with P_{app} values of around 4 nm/s. This is in line with previously reported LY P_{app} values of <6 nm/s in polarized MDCKII monolayers as evidence of good tight junction integrity (Irvine et al., 1999).

To examine bABCG2 secretory activity, we determined vectorial transepithelial transport of $MNPSO_2$. The MNP metabolite serves as the marker residue for drug disposition and residue studies in ruminants, including in milk (EMA, 2013). Besides, $MNPSO_2$ possesses a similar anthelmintic efficacy in vitro compared with the parent drug MNP (Karadzovska et al., 2009). Hence, the MNP metabolite $MNPSO_2$ serves as a suitable ABCG2 model substrate for representative examination of ABCG2-mediated drug transport in the bovine mammary gland. In agreement with apical bABCG2 membrane localization in MDCKII cells, we observed a preferential apically directed (B > A) saturable $MNPSO_2$ transport across the cell monolayer that resulted in a high $MNPSO_2$ efflux ratio (B > A/A > B) up to 8. A substance is considered a potential efflux transporter substrate if the efflux ratio is ≥2 in an epithelial cell system that exhibits efflux carrier expression, including ABCG2 (Giacomini et al., 2010). Moreover, in bABCG2-transduced MDCKII cells the ABCG2 inhibitor FTC reduced the $MNPSO_2$ efflux ratio by more than 50% to the mock-control level. Therefore, our data overall fulfill the requirement to demonstrate specific bABCG2-mediated $MNPSO_2$ transport (Giacomini et al., 2010).

In the MDCKII-mock cell line, an efflux ratio higher than 2 was observed, suggesting $MNPSO_2$ transport by endogenous canine ABCG2. However, FTC had no significant effect on the ER of $MNPSO_2$ in these cells. We therefore cannot exclude the contribution of other endogenously expressed ATP-binding cassette efflux transporters in the $MNPSO_2$ net flux in our MDCKII cell culture model. However, it was shown previously that expression of the efflux transporters P-glycoprotein, Mrp1, and Mrp2 was absent in the murine lactating mammary gland (Jonker et al., 2005). In contrast, we and others have shown that ABCG2 expression was highly increased in lactating ruminants (Jonker et al., 2005, Lindner et al., 2013). However, in the lactating mammary gland of dairy cows, contribution of efflux transporters other than ABCG2 in active drug secretion cannot be excluded.

In subsequent mechanistic studies, we aimed to elucidate the overall contribution of bABCG2 in secretion and concentration of therapeutically relevant drugs in milk. Therefore, we tested the interaction of ENRO, OXF, and MXD with bABCG2 by $MNPSO_2$ flux assays. In MDCKII-bABCG2 cells, all tested drugs significantly decreased the ER of $MNPSO_2$ nearly to the mock-control level. No relevant ER alteration was observed in mock cells. Concordantly, previous studies in the MDCKII-bABCG2 cell line (Wassermann et al., 2013b) or in MDCKII cells transduced with ABCG2 from bovine liver (Real et al., 2011) indicated ENRO transport by ABCG2. In regard to OXF, flux studies using murine ABCG2-transduced MDCKII monolayers showed a preferential apically directed (B > A) drug transport (Merino et al., 2005). In contrast, no net OXF flux could be detected in human P-glycoprotein- or multidrug resistance–associated protein 2–transduced MDCKII cell lines (Merino et al., 2005). MXD was previously identified as a murine ABCG2 substrate using *abcg2*$^{-/-}$ mice (Perez et al., 2009). In line with murine ABCG2 anthelmintic substrate specificity, our preliminary screening assays in MDCKII-bABCG2 cells indicated the interaction of OXF and MXD with bABCG2 (Wassermann et al., 2013a). Concordantly, PK studies in lactating sheep and buffalos reported high MXD M/P ratios (Imperiale et al., 2004; Dupuy et al., 2008), indicating active drug secretion into milk. Hence, our data altogether strongly indicated that therapeutically significant antibiotic and anthelmintic drugs interact with bABCG2. However, it is not possible to predict potential drug-drug interactions in our mechanistic studies, but as OXF and ENRO (Wassermann et al., 2013a, b; Halwachs et al., 2014) were shown to be bABCG2 substrates, drug-drug interactions may probably occur.

Lactation-induced bABCG2 expression may therefore result in active drug accumulation in milk as shown in our PK study for the active MNP metabolite $MNPSO_2$. The newly developed MNP exhibits a novel anthelmintic mode of action (Karadzovska et al., 2009) and is thereby of major importance as resistance of nematodes to other classes of anthelmintics increases in cattle (Behnke et al., 2008). Hence, our data on the pharmacokinetic behavior of $MNPSO_2$ is relevant for the interpretation of future MNP efficacy and residue studies in dairy cattle, including studies of drug secretion into milk. In the transport studies, selected $MNPSO_2$ and MXD concentrations were in the same range as C_{max} milk levels of $MNPSO_2$ in dairy cows and of MXD in dairy sheep (Imperiale et al., 2004). Besides, combination of different anthelmintic drugs including the tested substances is thought to be a valuable strategy to optimize therapeutic efficacy and to delay the development of anthelmintic resistance in ruminants (Lanusse et al., 2014). Therefore, our results may have implications for the pharmacotherapy of dairy animals, including potential drug-drug interactions among bABCG2 drug substrates. Additionally, our data may contribute to a better understanding of active drug residue formation in milk and thereby help to improve protection for the consumer of dairy products.

Acknowledgments

The authors thank C. Lakoma and B. Scholz for skillful technical assistance, L. Kuhnert for remarkable support, and Novartis Animal Health for providing MNP and $MNPSO_2$ pure analytical standards that were used for the analytical procedures within the PK studies.

Authorship Contributions

Participated in research design: Halwachs, Ballent, Imperiale, Lifschitz, Lanusse.

Conducted experiments: Mahnke, Ballent, Lifschitz.

Contributed new reagents or analytic tools: Ballent, Imperiale, Lifschitz, Baumann.

Performed data analysis: Mahnke, Halwachs, Ballent, Imperiale, Lifschitz, Baumann.

Wrote or contributed to the writing of the manuscript: Mahnke, Halwachs, Ballent, Lifschitz, Lanusse, Baumann, Honscha, von Bergen.

References

Alvarez AI, Merino G, Molina AJ, Pulido MM, McKellar QA, and Prieto JG (2006) Role of ABC transporters in veterinary drug research and parasite resistance. *Curr Drug Deliv* **3**: 199–206.

Behnke JM, Buttle DJ, Stepek G, Lowe A, and Duce IR (2008) Developing novel anthelmintics from plant cysteine proteinases. *Parasit Vectors* **1**:29.

Cho MJ, Thompson DP, Cramer CT, Vidmar TJ, and Scieszka JF (1989) The Madin Darby canine kidney (MDCK) epithelial cell monolayer as a model cellular transport barrier. *Pharm Res* **6**:71–77.

Doyle LA, Yang W, Abruzzo LV, Krogmann T, Gao Y, Rishi AK, and Ross DD (1998) A multidrug resistance transporter from human MCF-7 breast cancer cells. *Proc Natl Acad Sci USA* **95**:15665–15670.

Dupuy J, Sutra JF, Alvinerie M, Rinaldi L, Veneziano V, Mezzino L, Pennacchio S, and Cringoli G (2008) Plasma and milk kinetic of eprinomectin and moxidectin in lactating water buffaloes (Bubalus bubalis). *Vet Parasitol* **157**:284–290.

European Medicines Agency (EMA) (2013) European public MRL assessment report (EPMAR) for monepantel (extension to ovine milk) EMA/CVMP/741250/2011. Available online:http://www.ema.europa.eu/docs/en_GB/document_library/Maximum_Residue_Limits _-_ Report/2013/05/WC500143639.pdf.

Giacomini KM, Huang SM, Tweedie DJ, Benet LZ, Brouwer KL, Chu X, Dahlin A, Evers R, Fischer V, and Hillgren KM, et al.; International Transporter Consortium (2010) Membrane transporters in drug development. *Nat Rev Drug Discov* **9**:215–236.

Halwachs S, Wassermann L, Lindner S, Zizzadoro C, and Honscha W (2013) Fungicide prochloraz and environmental pollutant dioxin induce the ABCG2 transporter in bovine mammary epithelial cells by the arylhydrocarbon receptor signaling pathway. *Toxicol Sci* **131**: 491–501.

Halwachs S, Wassermann L, and Honscha W (2014) A novel MDCKII in vitro model for assessing ABCG2-drug interactions and regulation of ABCG2 transport activity in the caprine mammary gland by environmental pollutants and pesticides. *Toxicol In Vitro* **28**: 432–441.

Hegedus C, Szakács G, Homolya L, Orbán TI, Telbisz A, Jani M, and Sarkadi B (2009) Ins and outs of the ABCG2 multidrug transporter: an update on in vitro functional assays. *Adv Drug Deliv Rev* **61**:47–56.

Hosking BC, Stein PA, Karadzovska D, House JK, Seewald W, and Giraudel JM (2010) Effect of route of administration on the efficacy and pharmacokinetics of an experimental formulation of the amino-acetonitrile derivative monepantel in sheep. *Vet Rec* **166**:490–494.

Imperiale F, Lifschitz A, Sallovitz J, Virkel G, and Lanusse C (2004) Comparative depletion of ivermectin and moxidectin milk residues in dairy sheep after oral and subcutaneous administration. *J Dairy Res* **71**:427–433.

Irvine JD, Takahashi L, Lockhart K, Cheong J, Tolan JW, Selick HE, and Grove JR (1999) MDCK (Madin-Darby canine kidney) cells: A tool for membrane permeability screening. *J Pharm Sci* **88**:28–33.

Ito S and Lee A (2003) Drug excretion into breast milk–overview. *Adv Drug Deliv Rev* **55**: 617–627.

Jonker JW, Merino G, Musters S, van Herwaarden AE, Bolscher E, Wagenaar E, Mesman E, Dale TC, and Schinkel AH (2005) The breast cancer resistance protein BCRP (ABCG2) concentrates drugs and carcinogenic xenotoxins into milk. *Nat Med* **11**:127–129.

Karadzovska D, Seewald W, Browning A, Smal M, Bouvier J, and Giraudel JM (2009) Pharmacokinetics of monepantel and its sulfone metabolite, monepantel sulfone, after intravenous and oral administration in sheep. *J Vet Pharmacol Ther* **32**:359–367.

Kneuer C, Honscha KU, and Honscha W (2005) Rat reduced-folate carrier-1 is localized basolaterally in MDCK kidney epithelial cells and contributes to the secretory transport of methotrexate and fluoresceinated methotrexate. *Cell Tissue Res* **320**:517–524.

Krishnamurthy P and Schuetz JD (2006) Role of ABCG2/BCRP in biology and medicine. *Annu Rev Pharmacol Toxicol* **46**:381–410.

Lanusse C, Alvarez L, and Lifschitz A (2014) Pharmacological knowledge and sustainable anthelmintic therapy in ruminants. *Vet Parasitol* **204**:18–33.

Lifschitz A, Ballent M, Virkel G, Sallovitz J, Viviani P, and Lanusse C (2014) Accumulation of monepantel and its sulphone derivative in tissues of nematode location in sheep: pharmacokinetic support to its excellent nematodicidal activity. *Vet Parasitol* **203**:120–126.

Lindner S, Halwachs S, Wassermann L, and Honscha W (2013) Expression and subcellular localization of efflux transporter ABCG2/BCRP in important tissue barriers of lactating dairy cows, sheep and goats. *J Vet Pharmacol Ther* **36**:562–570.

Merino G, Jonker JW, Wagenaar E, Pulido MM, Molina AJ, Alvarez AI, and Schinkel AH (2005) Transport of anthelmintic benzimidazole drugs by breast cancer resistance protein (BCRP/ABCG2). *Drug Metab Dispos* **33**:614–618.

Perez M, Blazquez AG, Real R, Mendoza G, Prieto JG, Merino G, and Alvarez AI (2009) In vitro and in vivo interaction of moxidectin with BCRP/ABCG2. *Chem Biol Interact* **180**:106–112.
Perrier D and Gibaldi M (1982) General derivation of the equation for time to reach a certain fraction of steady state. *J Pharm Sci* **71**:474–475.
Rabindran SK, Ross DD, Doyle LA, Yang W, and Greenberger LM (2000) Fumitremorgin C reverses multidrug resistance in cells transfected with the breast cancer resistance protein. *Cancer Res* **60**:47–50.
Real R, González-Lobato L, Baro MF, Valbuena S, de la Fuente A, Prieto JG, Alvarez AI, Marques MM, and Merino G (2011) Analysis of the effect of the bovine adenosine triphosphate-binding cassette transporter G2 single nucleotide polymorphism Y581S on transcellular transport of veterinary drugs using new cell culture models. *J Anim Sci* **89**:4325–4338.
Stuchlíková L, Jirásko R, Vokřál I, Lamka J, Spulák M, Holčapek M, Szotáková B, Bártíková H, Pour M, and Skálová L (2013) Investigation of the metabolism of monepantel in ovine hepatocytes by UHPLC/MS/MS. *Anal Bioanal Chem* **405**:1705–1712.
Tsiboukis D, Sazakli E, Jelastopulu E, and Leotsinidis M (2013) Anthelmintics residues in raw milk. Assessing intake by a children population. *Pol J Vet Sci* **16**:85–91.
van Herwaarden AE and Schinkel AH (2006) The function of breast cancer resistance protein in epithelial barriers, stem cells and milk secretion of drugs and xenotoxins. *Trends Pharmacol Sci* **27**:10–16.
Wassermann L, Halwachs S, Lindner S, Honscha KU, and Honscha W (2013a) Determination of functional ABCG2 activity and assessment of drug-ABCG2 interactions in dairy animals using a novel MDCKII in vitro model. *J Pharm Sci* **102**:772–784.
Wassermann L, Halwachs S, Baumann D, Schaefer I, Seibel P, and Honscha W (2013b) Assessment of ABCG2-mediated transport of xenobiotics across the blood-milk barrier of dairy animals using a new MDCKII in vitro model. *Arch Toxicol* **87**:1671–1682.

Address correspondence to: Dr. Walther Honscha, Institute of Pharmacology, Pharmacy and Toxicology, Faculty of Veterinary Medicine, An den Tierkliniken 15, University of Leipzig, 04103 Leipzig, Germany. E-mail: honscha@vetmed.uni-leipzig.de